

1 **Contribution of carbonyl chromophores to secondary brown carbon from nighttime**
2 **oxidation of unsaturated heterocyclic volatile organic compounds**

3

4 Kunpeng Chen,¹ Raphael Mayorga,² Caitlin Hamilton,² Roya Bahreini,¹ Haofei Zhang,² Ying-
5 Hsuan Lin^{1,*}

6

7 ¹Department of Environmental Sciences, University of California, Riverside, California 92521,
8 United States

9 ²Department of Chemistry, University of California, Riverside, California 92521, United States

10

11

12

13

14

15

16

17

18

19

20

21 **ABSTRACT**

22 The light absorption properties of brown carbon (BrC), which are linked to molecular
23 chromophores, may play a significant role in the Earth's energy budget. While nitroaromatic
24 compounds have been identified as strong chromophores in wildfire-driven BrC, other types of
25 chromophores remain to be investigated. As an electron-withdrawing group ubiquitous in the
26 atmosphere, we characterized carbonyl chromophores in BrC samples from the nighttime
27 oxidation of furan and pyrrole derivatives, which are important but understudied precursors of
28 secondary organic aerosols (SOA) primarily found in wildfire emissions. Various carbonyl
29 chromophores were characterized and quantified in BrC samples, and their ultraviolet-visible (UV-
30 Vis) spectra were simulated using time-dependent density functional theory (TD-DFT). Our
31 findings suggest that chromophores with carbonyls bonded to nitrogen (i.e., imides and amides)
32 derived from N-containing heterocyclic precursors substantially contribute to BrC light absorption.
33 The quantified N-containing carbonyl chromophores contributed to over 40% of the total light
34 absorption at wavelengths below 350 nm and above 430 nm in pyrrole BrC. The contributions of
35 chromophores to total light absorption differed significantly by wavelength, highlighting their
36 divergent importance in different wavelength ranges. Overall, our findings highlight the
37 significance of carbonyl chromophores in secondary BrC and underscore the need for further
38 investigation.

39

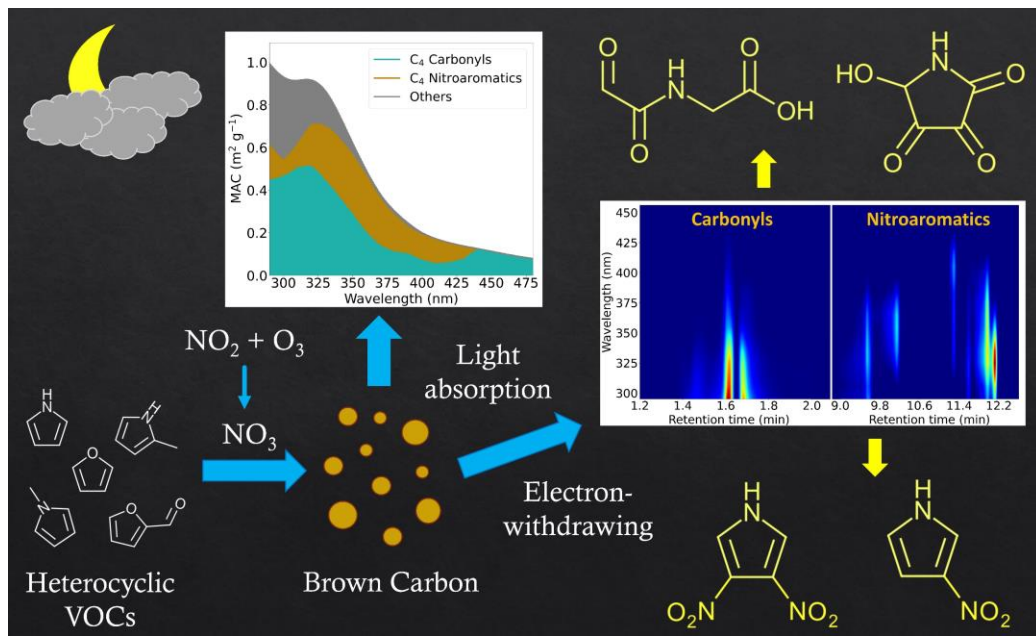
40 **KEYWORDS**

41 furan and pyrrole derivatives, secondary organic aerosols, imides and amides, light absorption
42 contribution, wavelength dependency

43

44 **Synopsis**

45 Atmospheric carbonyls are formed by the oxidation of various volatile organic compounds (VOCs),
46 and they have the potential to be important chromophores in secondary brown carbon, especially
47 those from nighttime oxidation of N-containing heterocyclic VOC precursors.



51 **INTRODUCTION**

52 Atmospheric brown carbon (BrC) is an important contributor to global warming, with a
53 $+0.10\text{-}0.55 \text{ W m}^{-2}$ direct radiative effect¹⁻³ ($\sim 20\text{-}24\%$ contribution) on the top-of-atmosphere direct
54 radiative forcing.^{4, 5} The contribution of BrC absorption is enhanced at higher altitudes⁶ and varies
55 by both daily and seasonal cycles,⁷ especially due to changes in air pollution and cloud coverage.⁷
56 ⁸ Conversely, the light absorption of BrC may also indirectly reduce the global coverage of clouds
57 and decrease their cooling effects.⁹ The spatial and temporal variations of BrC light absorption,
58 and consequently their impacts, are strongly related to the changes in chemical composition.^{8, 10}
59 However, parameterization pertinent to BrC constituents remains underdeveloped in climate
60 models,¹¹ hindering accurate evaluations of BrC optical properties and climate change prediction.^{12,}
61 ¹³

62 Accurate representations of BrC's effects on climate change require a comprehensive
63 process-level understanding of the formation and evolution of molecular chromophores, which
64 play a key role in regulating the light absorption properties of BrC. Nitroaromatic chromophores,
65 also known as nitrated aromatic compounds, have been recognized as significant contributors to
66 BrC light absorption. For example, Li et al. and Frka et al. reported that nitroaromatic
67 chromophores may contribute to $\sim 17\text{-}31\%$ light absorption of BrC at 365-370 nm,^{14, 15} while
68 Bluvshtein et al. and Lin et al. indicated an even higher ratio (i.e., 50-80%) at wavelengths above
69 350 nm in biomass burning events.^{16, 17} Although nitroaromatic chromophores may not account
70 for a large fraction of aerosol mass, their contribution to BrC light absorption at 365 nm can be
71 $\sim 2\text{-}10$ times that of their mass contribution in BrC samples.^{14, 15, 18, 19} Among a variety of
72 nitroaromatic chromophores, nitrophenols and nitrocatechols have been identified as two major
73 groups of nitroaromatic chromophores in ambient aerosols,^{19, 20} and they have been widely

74 investigated to characterize the BrC formation and evolution due to photooxidation or
75 photolysis.²¹⁻²⁶

76 While nitroaromatic chromophores have been identified as potential tracers of BrC in
77 atmospheric processing due to their significant role in the light absorption of BrC at 365 nm,²⁷ the
78 contributors to the BrC absorption spectra in the near ultraviolet (UV) range below 365 nm have
79 not been fully deconvoluted. In contrast to the >50% contribution of light absorption above 350
80 nm, nitroaromatic chromophores only accounted for ~20% of light absorption at 300 nm in
81 biomass burning events, according to studies reported by Bluvshtein et al. and Lin et al.^{16, 17} The
82 wavelength-dependent contributions to BrC light absorption suggest the critical role of other types
83 of chromophores in UV absorption. Since the light absorption of BrC chromophores is induced by
84 electronic transitions, similar to nitroaromatics, which have strongly electron-withdrawing nitro
85 groups attached to the aromatic rings, unsaturated organic compounds or conjugated systems
86 coupled with other types of electron-withdrawing groups such as carbonyls could also be
87 chromophore candidates.^{13, 28} For instance, the simplest unsaturated carbonyl compound (i.e.,
88 acrolein) can absorb sunlight above 290 nm.^{29, 30} From field studies, it has been reported that
89 carbonyls may contribute to a large mass fraction of biomass burning aerosols^{31, 32} and significant
90 light absorption in the BrC.^{10, 33, 34} The molecular absorptivity of numerous carbonyl compounds
91 observed in ambient aerosols is comparable to the absorptivity of nitroaromatic chromophores at
92 290-350 nm.³⁵ Therefore, it is essential to characterize carbonyl chromophores and constrain their
93 roles in BrC light absorption.

94 In this study, we characterized carbonyl chromophores in secondary organic aerosols (SOA)
95 from the nighttime oxidation of a series of unsaturated heterocyclic volatile organic compounds
96 (VOCs), including pyrrole, 1-methylpyrrole (1-MP), 2-methylpyrrole (2-MP), furan, and furfural,

97 that have been widely observed in biomass burning events,³⁶⁻⁴⁰ and may account for ~30% of the
98 initial nitrate radical (NO_3) reactivity in wildfire-driven nighttime chemistry.⁴⁰ Recently, these
99 VOCs were reported as potentially important precursors for secondary BrC formation during
100 nighttime oxidation,⁴¹⁻⁴⁴ in which several carbonyl chromophores were observed.⁴³ Multi-
101 instrumental characterization along with theoretical calculations of ultraviolet-visible (UV-Vis)
102 spectra were employed here to elucidate the structures of carbonyl chromophores and their spectral
103 light absorptivity. This study focuses on the light absorption contribution of carbonyl
104 chromophores in pyrrole SOA and 2-MP SOA; because nitroaromatic chromophores have been
105 identified as critical contributors to BrC light absorption in these systems, they can serve as a
106 benchmark for comparisons.⁴² Characterizing BrC chromophores at the molecular level can
107 contribute to a deeper process-level understanding of the formation and evolution of secondary
108 BrC light absorption in changing environments.

109

110 METHODS

111 **Experimental setup.** Experiments were performed in a 10 m³ Teflon FEP chamber at room
112 temperature (20-25 °C) and low relative humidity (RH< 20%) in the dark. Details of the
113 experimental setup and SOA properties, including number and size distribution, aerosol effective
114 density, and mass fraction of organics, were introduced in our previous studies.^{42, 43} In brief, 450
115 ppb NO_2 and 1500 ppb O_3 (initial $[\text{NO}_2]/[\text{O}_3] = 0.3$) were first injected into the chamber and
116 allowed to react for one hour, producing ~22 ppb nitrate radicals (NO_3).⁴² To investigate the effects
117 of NO_3 radical levels on the light absorption contributions of BrC chromophores, additional
118 experiments were carried out with 150 ppb NO_2 and 1500 ppb O_3 (initial $[\text{NO}_2]/[\text{O}_3] = 0.1$),
119 producing ~8 ppb NO_3 .⁴² The concentrations of NO_2 and O_3 were monitored by a NO_x analyzer

120 (Teledyne Instruments) and an O₃ analyzer (Advanced Pollution Instrumentation, Inc.),
121 respectively. Our previous studies indicated that the nighttime oxidation of pyrroles and furans
122 under both conditions was predominantly initiated by NO₃ radicals.^{42, 44} After the one-hour
123 reaction between O₃ and NO₂ to produce NO₃ radicals, one of the studied heterocyclic VOCs was
124 first vaporized in a heated jar and then injected into the chamber with ~15 lpm of nitrogen gas.
125 The target concentration of VOCs in the chamber was ~200 ppb. After the mass concentration
126 reached a plateau, the generated SOA particles were collected on polytetrafluoroethylene (PTFE)
127 membrane filters (46.2 mm, 2.0 μ m, Tisch Scientific) for one hour with a flowrate of 16.7 lpm;
128 each filter collected the aerosols from 1 m³ of chamber air and served for subsequent offline
129 analysis. Although chamber experiments have some limitations in simulating the real atmosphere
130 (e.g., size-dependent particulate wall loss rate (Fig. S1) that may affect the chromophore
131 quantification),⁴⁵ the controlled chamber conditions can systematically facilitate the
132 characterization of carbonyl chromophores and the evaluation of their roles in secondary BrC.

133 **Compositional analysis.** The compositional analysis was conducted using a suite of
134 complementary analytical instruments. A liquid chromatography coupled with a diode array
135 detector, an electrospray ionization source (negative ion mode), and a quadrupole-time-of-flight
136 tandem mass spectrometer (LC-DAD-ESI(-)-Q-TOFMS, Agilent Technologies 1260 Infinity II,
137 and 6545 Q-TOF LC/MS) was used to identify light-absorbing carbonyl products and to
138 characterize their molecular structures. The gradient elution for the changing LC mobile phase
139 composition over time is shown in Fig. S2A. A gas chromatography-electron ionization mass
140 spectrometry (GC/EI-MS, Agilent Technologies 6890N GC System, and 5975 inert XL Mass
141 Selective Detector) was also used to complementarily identify carbonyl products. An iodide-
142 adduct time-of-flight chemical ion mass spectrometry coupled with the Filter Inlet for Gases and

143 AEROSols system (FIGAERO-ToF-CIMS, Aerodyne Research Inc.)⁴⁶ and an ion mobility
144 spectrometry time-of-flight mass spectrometer (IMS-TOF, Tofwerk Inc.) were used to characterize
145 SOA composition in real time and offline, respectively. All the characterization methods were the
146 same as those in our prior studies.^{42, 43} Detailed instrumental setups and operational parameters
147 have been described previously.^{42, 43, 47-49}

148 N-containing carbonyl chromophores were characterized by LC-DAD-ESI-Q-TOFMS and
149 GC/EI-MS, and their mass contributions were estimated semi-quantitatively using maleimide
150 ($C_4H_3NO_2$) as a surrogate standard. The mass ratio of the characterized N-containing carbonyl
151 chromophores ($MR_{carbonyl}$) (Eq. (1)), and the mass ratio of maleimide ($MR_{maleimide}$) in SOA samples
152 from pyrrole and its derivatives had been previously determined by GC/EI-MS using a similar
153 approach.⁴³

154
$$MR_{carbonyl} = MR_{maleimide} \frac{c_{carbonyl} M_{carbonyl}}{c_{maleimide} M_{maleimide}} = MR_{maleimide} R_F \frac{A_{carbonyl} M_{carbonyl}}{A_{maleimide} M_{maleimide}} \quad (1)$$

155 Here, $c_{carbonyl}$ and $c_{maleimide}$ are the molar concentrations of the characterized carbonyl
156 chromophores and maleimide in the extracted SOA samples ($mol\ L^{-1}$); $M_{carbonyl}$ and $M_{maleimide}$ are
157 the molar masses of the characterized carbonyl chromophores and maleimide in the extracted SOA
158 samples ($g\ mol^{-1}$); $A_{carbonyl}$ and $A_{maleimide}$ are the peak areas of parent ions of the characterized
159 carbonyl chromophores and maleimide in their extracted ion chromatograms (EICs) measured by
160 LC-DAD-ESI-Q-TOFMS. Although response factors (R_F) of the characterized N-containing
161 carbonyl chromophores may differ slightly from the surrogate standard (Fig. S2B), semi-
162 quantification can provide approximate mass ratios and still support comparisons of the
163 representation of various N-containing carbonyl chromophores in SOA samples.

164

165 **Light absorption measurements.** The absorbance of SOA samples (290-700 nm) was measured
166 by a UV-Vis spectrophotometer (Beckman DU-640). The SOA mass on each filter sample varied
167 within 10-350 μg , depending on the type of VOCs. Each filter sample was extracted with 22 mL
168 of acetonitrile (ACN), which has been shown to be a suitable solvent for the analysis of secondary
169 BrC due to its chemical stability (aprotic) and solubility for polar compounds.⁴³ It is noted that
170 ACN may not completely extract the SOA constituents from filters (Table S1), so the BrC light
171 absorption estimated in this study is the lower limit. The contribution of BrC carbonyl marker
172 compounds (i.e., maleimide and phthalic anhydride)⁴³ to the total light absorption of SOA samples
173 ($AbsC$), which can vary greatly with wavelength (λ), is estimated by Eq. (2).

174

$$AbsC(\lambda) = \frac{Abs_{chro}(\lambda)}{Abs_{BrC}(\lambda)} \quad (2)$$

175 $Abs_{BrC}(\lambda)$ is the total light absorbance of the BrC samples, directly measured by the UV-
176 Vis spectrophotometer, while $Abs_{chro}(\lambda)$ is the light absorbance of the investigated BrC
177 chromophores, calculated by the Beer-Lambert law (Eq. (3)).

178

$$Abs_{chro}(\lambda) = \varepsilon_{chro}(\lambda) \times \frac{m_{chro}}{M_{chro}} \times b \quad (3)$$

179 $\varepsilon_{chro}(\lambda)$ is the molecular absorptivity of the investigated BrC chromophores ($\text{L mol}^{-1} \text{cm}^{-1}$),
180 which has been reported in our previous work;⁴³ m_{chro} is the mass concentration of molecular
181 chromophores in the SOA solution samples ($\text{ng } \mu\text{L}^{-1}$); M_{chro} is the molar mass of the molecular
182 chromophores (g mol^{-1}); and b is the instrumental light path (i.e., 1 cm).

183 **Computations of theoretical UV-Vis spectra.** The time-dependent density functional theory
184 (TD-DFT) was used to simulate the wavelength-dependent light absorptivity of the characterized
185 carbonyl products, for which no authentic standards were available. The Gaussian 16 program
186 (revision C. 01)⁵⁰ was used for all computations, with the B3LYP functional^{51, 52} and the 6-

187 311++G(d,p) basis set⁵³ as suggested in previous studies.^{54, 55} The ACN solvent environment was
188 simulated by the integral equation formalism extension of the polarizable continuum model
189 (IEFPCM).⁵⁶ The GaussView 6 program was used to generate the theoretical UV-Vis spectra. All
190 the Cartesian coordinates for geometrical structures were summarized in Table S2.

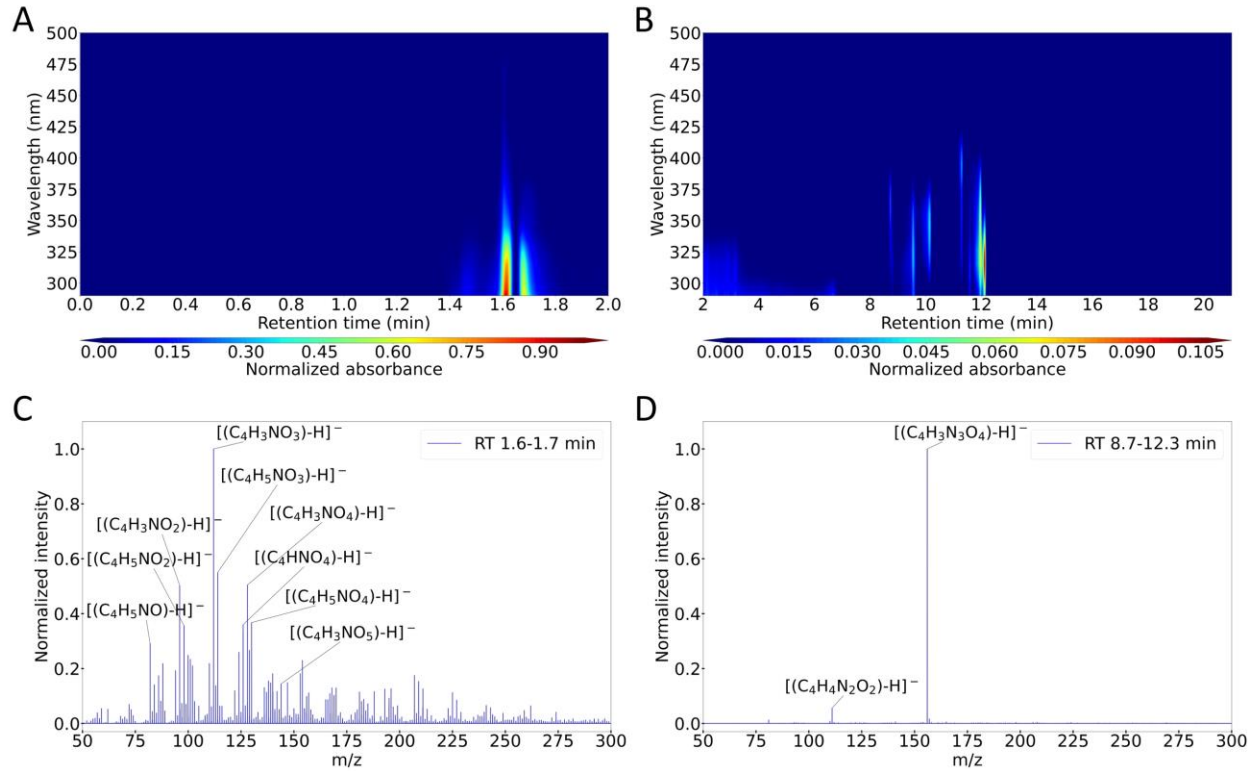
191

192 RESULTS AND DISCUSSIONS

193 **Distribution of chromophores in the LC-DAD heatmaps.** The LC-DAD heatmaps provide a
194 snapshot of BrC chromophore distributions for all the SOA samples (Fig. 1 and Figs. S3-5), where
195 the hotspots illustrate the retention time (RT) and wavelengths of light absorption. Fig. 1 shows
196 the LC-DAD heatmap of pyrrole SOA, which is divided into two panels, corresponding to the RT
197 ranges of 0-2 min and 2-21 min, respectively (Fig. 1A-B).

198 Compositional analysis revealed that the major hotspots detected at RT of 1.6-1.7 min may
199 be attributed to mono-nitrogen chromophores (Fig. 1C), while those detected at RT of 8.7-12.3
200 min may be ascribed to the di-nitrogen and tri-nitrogen chromophores (Fig. 1D). Notably, the
201 analytes at RT of 1.6-1.7 min were comprised of many mono-nitrogen compounds, while only two
202 products were shown at RT of 8.7-12.3 min. The mono-nitrogen chromophores (Fig. 1A) in pyrrole
203 SOA collectively acquired much stronger light absorption compared to di-nitrogen and tri-nitrogen
204 chromophores (Fig. 1B), which indicated the potential importance of the mono-nitrogen
205 chromophores in BrC light absorption. The strong light absorption corresponding to mono-
206 nitrogen chromophores is also observed in 1-MP SOA (Fig. S3) and 2-MP SOA (Fig. S4), wherein
207 the mono-nitrogen chromophores led to much higher or similar absorption intensities compared to
208 those of the di-nitrogen and tri-nitrogen chromophores. In a recent study, we found di-nitrogen
209 and tri-nitrogen chromophores in pyrrole SOA and 2-MP SOA as nitro- and dinitro-substituted

210 chromophores.⁴² This finding suggested that the mono-nitrogen chromophores would lack nitro
211 groups, and their nitrogen may be inherited from the pyrrole backbones, as evidenced by the
212 structural characterization in the following section. However, in contrast to electron-withdrawing
213 groups such as nitro groups, the nitrogen atom on the pyrrole backbone cannot attract electron
214 density toward itself and thus the light absorption of the mono-nitrogen chromophores is mostly
215 due to the non-nitrogen electron-withdrawing groups in the molecule. Furthermore, our previous
216 study of furan SOA revealed that nitrogen-free products were the predominant contributors to the
217 major LC-DAD hotspots,⁴⁴ whereas the major hotspots in furfural SOA can be attributed to both
218 nitrogen-containing and nitrogen-free products (Fig. S5). Despite this, all the LC-DAD heatmaps
219 indicate the importance of different types of electron-withdrawing groups in BrC light absorption.
220 Analysis of functional groups with attenuated total reflectance Fourier-transform infrared (ATR-
221 FTIR) spectroscopy conducted in our previous study suggested that chromophores with carbonyl
222 groups may account for a significant portion of the light absorption of SOA samples from
223 nighttime oxidation of heterocyclic VOCs.⁴³



224 **Figure 1.** LC-DAD heatmaps of pyrrole SOA: (A) 0-2 min, and (B) 2-21 min, followed by the
 225 mass spectra corresponding to the major hotspots, respectively (C-D). The light absorption of
 226 chromophores was normalized to the highest value of the whole LC-DAD heatmap, with each
 227 panel having its own color scale for a clear representation of chromophore distribution. With LC
 228 mobile phase changing (Fig. S2A), the separated hotspots in two unique RT zones represent
 229 distinct chromophores with different polarities.
 230

231
 232 Even though nitroaromatic chromophores have been identified as important contributors
 233 to BrC light absorption in pyrrole SOA and 2-MP SOA,^{41, 42} the LC-DAD heatmaps (Fig. 1A-B
 234 and Fig. S3A-B) disclosed that mono-nitrogen chromophores could account for the majority of the
 235 light absorption. This is because nitroaromatic chromophores and mono-nitrogen chromophores

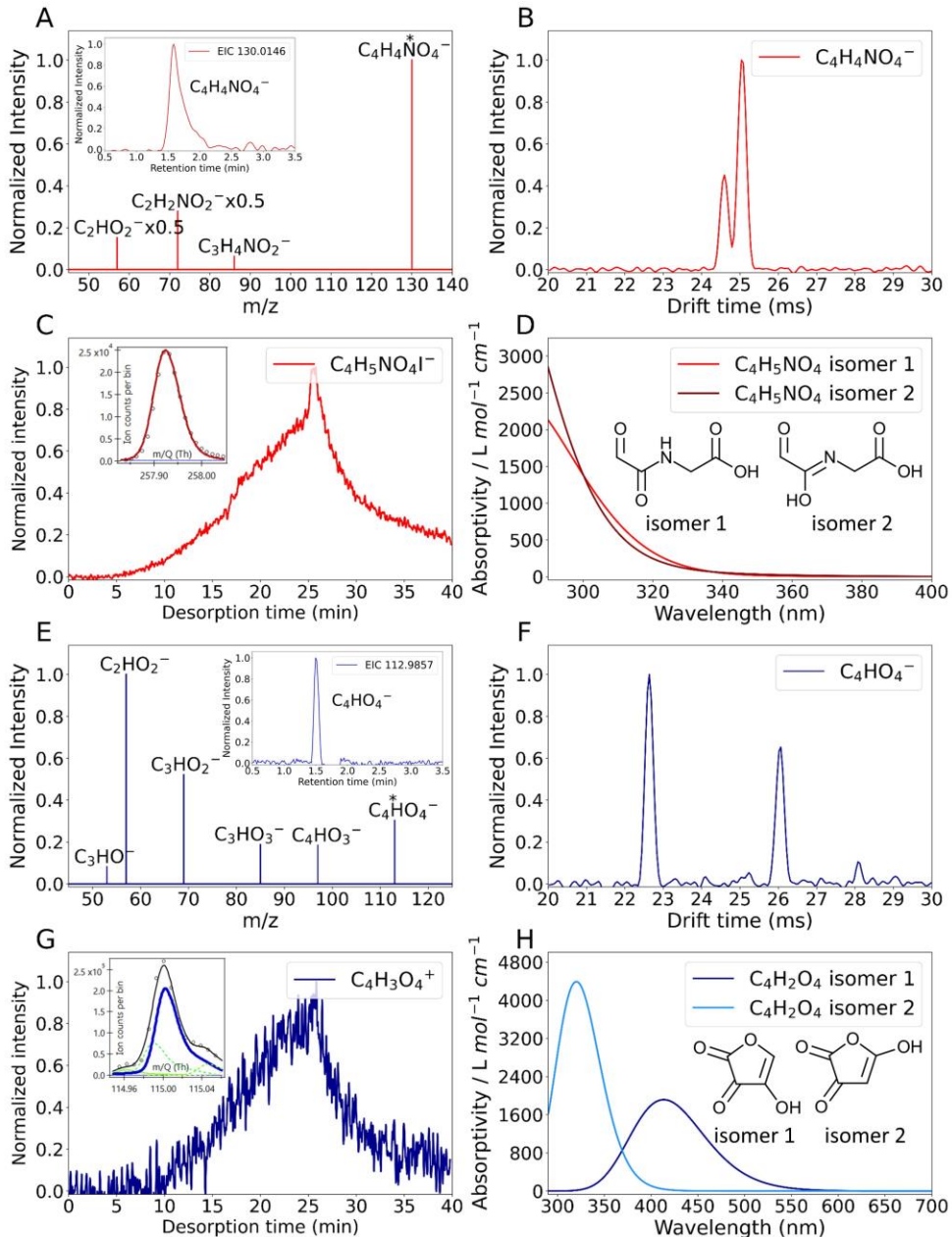
236 have absorption peaks at different wavelength ranges and, as a result, have wavelength-dependent
237 light absorption contributions, which will be discussed further in the following sections.

238

239 **Molecular characterization of carbonyl chromophores.** In the current study, the molecular
240 composition of carbonyl chromophores was determined by complementary analytical
241 instrumentation, and their UV-Vis spectra were simulated using quantum chemical approaches
242 (Figs. 2 and 3). Following the identification of the molecular formula in Fig. 1C, we performed
243 tandem MS experiments to elucidate their structures. Here, $\text{C}_4\text{H}_4\text{NO}_4^-$, a deprotonated ion of
244 $\text{C}_4\text{H}_5\text{NO}_4$, is selected as an example. The LC-ESI-Q-ToFMS measurements showed a single peak
245 in the EIC of this ion as well as its fragmentation pattern (Fig. 2A), which can help derive the
246 tentative molecular structures and thus support the theoretical computation of UV-Vis spectra. The
247 IMS-TOF measurements also confirmed the presence of $\text{C}_4\text{H}_4\text{NO}_4^-$ in ESI (-) and indicated two
248 major isomers for this ion (Fig. 2B). To rule out the potential interference from solvent and LC
249 electrospray ionization efficiency,^{43, 44} the presence of $\text{C}_4\text{H}_5\text{NO}_4$ was supplementally verified by
250 *in situ* characterization with FIGAERO-ToF-CIMS (Fig. 2C). Plausible fragmentation pathways
251 were derived based on the tandem MS data (Fig. S6A), wherein $\text{C}_4\text{H}_5\text{NO}_4$ can be characterized as
252 formyl carbonyl amino acetic acid and its imidic acid isomer. Both compounds are chain-structural
253 carbonyl chromophores, as confirmed by the theoretical computation of their UV-Vis spectra (Fig.
254 2D). Using the same approaches, the ring-retaining carbonyl chromophores in pyrrole SOA were
255 also characterized, including 2-hydroxy-2-pyrroline-4,5-dione ($\text{C}_4\text{H}_3\text{NO}_3$), 5-hydroxy-2,3,4-
256 pyrrolidinetrione ($\text{C}_4\text{H}_3\text{NO}_4$), and 5-hydroxy-2,3-pyrrolidinedione ($\text{C}_4\text{H}_5\text{NO}_3$) (Figs. S7-10).
257 Similar to pyrrole, nighttime oxidation of furan can generate light-absorbing diones. As one of the
258 major products in furan SOA, $\text{C}_4\text{H}_2\text{O}_4$ was characterized as 4-hydroxyfuran-2,3-dione and 5-

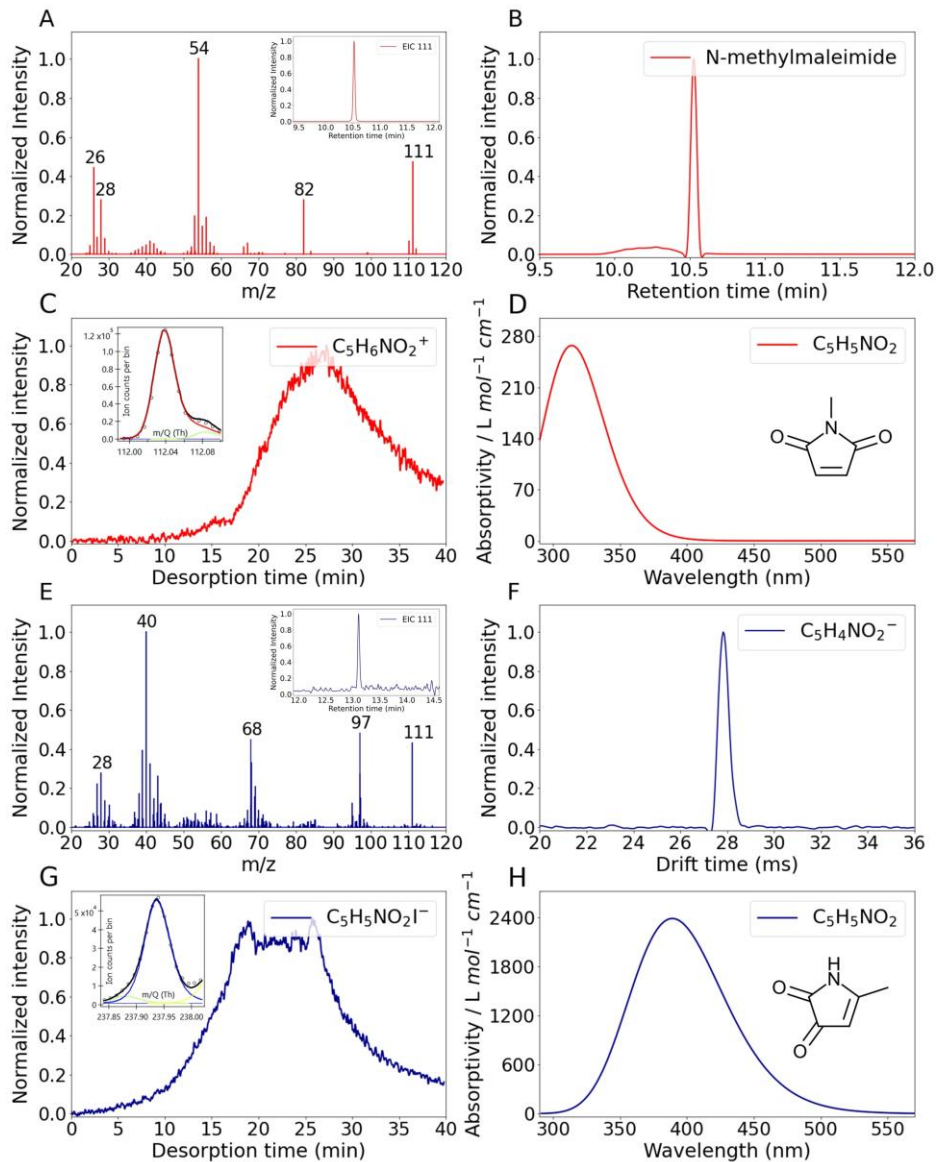
259 hydroxyfuran-2,3-dione (Figs. 2E-G and Fig. S6B).⁴⁴ These products exhibit distinct UV-Vis
260 spectra with different central wavelengths and peak absorptivity (Fig. 2H).

261 Given that both LC-ESI-Q-TOFMS and IMS-TOF in this study could only detect
262 deprotonated ions (because of the nature and limitations of ESI(-)) and may not characterize all
263 carbonyls generated, GC/EI-MS was used to investigate more diverse carbonyl chromophores.
264 Previous GC/EI-MS analysis of secondary BrC samples revealed a number of light-absorbing
265 heterocyclic diones, including maleimide (from pyrrole and its derivatives), maleic anhydride, and
266 phthalic anhydride (from furan and furfural).⁴³ In the current study, N-methylmaleimide was
267 discovered by GC/EI-MS (RT = 10.5 min) in 1-MP SOA samples (Fig. 3A). The presence of this
268 compound was confirmed by its authentic chemical standard (Fig. 3B) and also supported by the
269 tentative fragmentation pathways (Fig. S11A) as well as the *in situ* FIGAERO-ToF-CIMS
270 measurement (Fig. 3C). Also, the presence of 2-methyl-2-pyrroline-4,5-dione, an isomer of N-
271 methylmaleimide, in 2-MP SOA was confirmed by multi-instrumental measurements (Figs. 3E-G)
272 and the tentative fragmentation pathways (Fig. S11B). The calculated UV-Vis spectra showed that
273 both diones can contribute to light absorption above 290 nm (Figs. 3D and 3H).



274

275 **Figure 2.** Characterization of carbonyl chromophores in pyrrole SOA and furan SOA: (A) EICs
 276 and tandem mass spectra of $\text{C}_4\text{H}_5\text{NO}_4$; (B) IMS-TOF drift grams of $\text{C}_4\text{H}_5\text{NO}_4$; (C) FIGAERO-
 277 ToF-CIMS peak fitting and thermograms of $\text{C}_4\text{H}_5\text{NO}_4$; (D) theoretical UV-Vis spectra of isomers
 278 of $\text{C}_4\text{H}_5\text{NO}_4$; (E) EICs and tandem mass spectra of $\text{C}_4\text{H}_2\text{O}_4$; (F) IMS-TOF drift grams of $\text{C}_4\text{H}_2\text{O}_4$;
 279 (G) FIGAERO-ToF-CIMS peak fitting and thermograms of $\text{C}_4\text{H}_2\text{O}_4$; (H) theoretical UV-Vis
 280 spectra of $\text{C}_4\text{H}_2\text{O}_4$ isomers.



281

282 **Figure 3.** Characterization of carbonyl chromophores in 1-MP SOA and 2-MP SOA: (A) GC/EI-
 283 MS characterization of $\text{C}_5\text{H}_5\text{NO}_2$ in 1-MP SOA; (B) EIC of m/z 111 from the N-methylmaleimide
 284 chemical standard; (C) FIGAERO-ToF-CIMS peak fitting and thermograms of $\text{C}_5\text{H}_5\text{NO}_2$ in 1-MP
 285 SOA; (D) theoretical UV-Vis spectrum of $\text{C}_5\text{H}_5\text{NO}_2$ in 1-MP SOA; (E) GC/EI-MS
 286 characterization of $\text{C}_5\text{H}_5\text{NO}_2$ in 2-MP SOA; (F) IMS-TOF drift gram of $\text{C}_5\text{H}_5\text{NO}_2$ in 2-MP SOA;
 287 (G) FIGAERO-ToF-CIMS peak fitting and thermograms of $\text{C}_5\text{H}_5\text{NO}_2$ in 2-MP SOA; (H)
 288 theoretical UV-Vis spectrum of $\text{C}_5\text{H}_5\text{NO}_2$ in 2-MP SOA.

289

290 Notably, N-containing carbonyl chromophores such as imides and amides are ubiquitous
291 in SOA samples from the N-containing heterocyclic VOC precursors (e.g., pyrrole and its
292 derivatives in this study). The lone pair electrons from the nitrogen atom in imides and amides can
293 conjugate with the unsaturated bonds (e.g., carbonyl groups), which facilitate the $n-\pi^*$ excitation
294 of delocalized electrons and hence support the formation of BrC chromophores. However,
295 different N-containing carbonyl chromophores may lead to different contributions to BrC light
296 absorption, depending on their mass ratio in SOA samples, spectral wavelengths, and absorptivity.
297 For example, $C_4H_5NO_4$ and $C_4H_3NO_3$ have similar mass ratios in pyrrole SOA ($3.37\pm0.11\%$ and
298 $2.86\pm0.57\%$, respectively) based on the semi-quantification, but the UV-Vis spectrum of $C_4H_5NO_4$
299 only covers 290-350 nm (Fig. 2D), while the UV-Vis spectrum of $C_4H_3NO_3$ can extend to 500 nm
300 (Fig. S7J). Although the UV-Vis spectra of $C_4H_3NO_3$ and $C_4H_5NO_4$ cover a similar range of
301 wavelengths, the latter possesses a higher mass ratio ($8.86\pm1.11\%$) and a lower absorptivity (Fig.
302 S7K). It is also noted that the presence of nitrogen may lead to a redshift of the spectral peaks (e.g.,
303 Fig. S7J and isomer 2 in Fig. 2H), suggesting the potentially important role of N-containing
304 carbonyl chromophores in modulating BrC light absorption.

305

306 **Light absorption contribution of carbonyl and nitroaromatic chromophores.** The light
307 absorption contributions of identified carbonyl and nitroaromatic chromophores can be estimated
308 by comparing their integrated LC-DAD absorbance within the corresponding RT ranges to the
309 overall LC-DAD absorbance, which are similar to those described in the literature.^{16, 17} Although
310 the estimated light absorption contributions may not be rigorously accurate due to the incomplete
311 elution of chromophores that can strongly interact with the stationary phase of the LC column,¹⁷

312 this approach has successfully revealed the indispensable role of nitroaromatic chromophores in
313 BrC aerosols from biomass burning events.^{16, 17} Similarly, the relative importance of carbonyl
314 chromophores and nitroaromatic chromophores at different wavelengths can thus be evaluated by
315 this approach. Here, C₄ carbonyls and C₄ nitroaromatics in pyrrole SOA, which may
316 predominantly contribute to the major hotspots in the LC-DAD heatmaps (Fig. 1), were
317 categorized as two groups of chromophores, while other chromophores, which may comprise
318 oxidation products with higher molecular weights and high double bond equivalence (DBE) (Fig.
319 S12), were classified as “others.” It is noted that the C₄ N-containing carbonyls (both ring-retaining
320 and ring-opening products) and C₄ nitroaromatics are produced from the C₄ backbone of pyrrole;
321 in other VOC systems, the carbon number of the lower-molecular-weight chromophores can be
322 different and dependent on the VOC precursors. The light absorption contribution of each group
323 of chromophores was visualized along with the wavelengths in both percentages (Fig. S13A-B)
324 and mass absorption coefficient (MAC) profiles (Fig. 4). The latter was estimated by combining
325 Fig. S13 and the MAC profiles reported in our prior study.⁴²

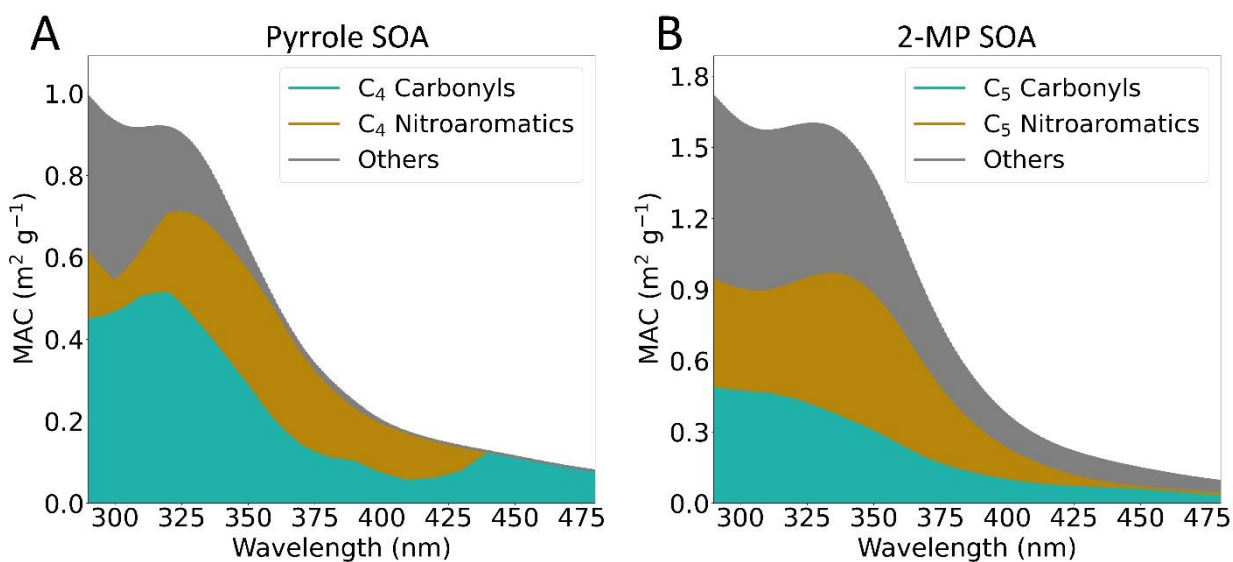
326 Our results showed that, while C₄ nitroaromatics account for the majority of light
327 absorption in the 350-430 nm range, C₄ carbonyls contribute significantly more below 350 nm and
328 above 430 nm, accounting for over 40% of the total light absorption in both wavelength ranges
329 (Fig. 4A and Fig. S13A). The C₅ nitroaromatics and C₅ carbonyls in 2-MP SOA, which are
330 produced from the C₅ backbone of 2-MP (Ref. 42 and Fig. 3H), revealed comparable tendencies
331 in the wavelength dependence of light absorption contribution (Fig. 4B and Fig. S13B). However,
332 in the visible range, the contribution of C₄ carbonyls to light absorption was greater than the other
333 two categories in pyrrole SOA (Fig. 4A and Fig. S13A), whereas the contributions of the three
334 categories in 2-MP SOA were comparable (Fig. 4B and Fig. S13B). The quantitative differences

335 between Fig. 4A and Fig. 4B (also between Fig. S13A and Fig. S13B) reveal the vital role of VOC
336 structures in regulating the relative contributions of carbonyl chromophores and nitroaromatic
337 chromophores to secondary BrC light absorption, which could be due to the interference of diverse
338 oxidation pathways (e.g., diverse pyrrolyl radical shifts).⁴²

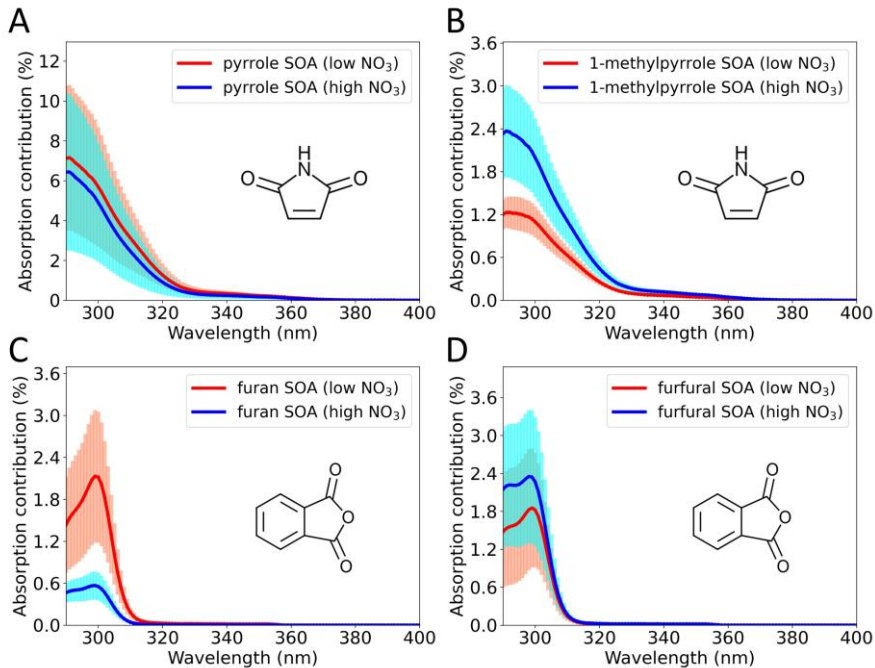
339 The relative impact of carbonyl chromophores on BrC light absorption is further evaluated
340 by the ratio of their absorption cross-section emission factors (EF_{absC}), which accounts not only
341 for the MACs but also the carbon emission factors of VOC precursors from burning sources and
342 the SOA yields.⁴¹ Details of the EF_{absC} calculations for pyrrole SOA and 2-MP SOA were
343 described previously.⁴² Taking biomass burning of ponderosa pine forests, which is relevant to
344 wildfires in the western US and Canada,⁵⁷ as an example, C₄₋₅ carbonyl chromophores may
345 contribute more to BrC light absorption below 350 nm and above 430 nm than C₄₋₅ nitroaromatic
346 chromophores (Table S3). It is also noted that the light absorption of 1-MP SOA was mainly
347 attributed to mono-nitrogen C₄₋₅ carbonyls and the “others” category instead of C₄₋₅ nitroaromatics
348 (Fig. 3D, Fig. S4, Fig. S14A, and Fig. S15A). As highlighted in our prior study,⁴² the absence of
349 C₄₋₅ nitroaromatics may account for the inhibited nitro-substitution by the methyl group on the
350 nitrogen atom of the 1-MP backbone, which reinforces the importance of VOC structures in the
351 light absorption contribution of carbonyl chromophores.

352 In addition, the heteroatoms in heterocyclic VOCs may greatly alter the oxidation pathways
353 and hence the light absorption contribution of carbonyl and nitroaromatic chromophores. For
354 example, formation of pyrrole-derived nitroaromatics is initiated by the H-abstraction on the
355 nitrogen heteroatom,⁴² while formation of furan-derived carbonyls is related to the NO₃ addition
356 and subsequent NO₂ elimination mechanisms affected by the oxygen heteroatom.⁵⁸ Our previous
357 research and the current findings suggest that the light absorption of furan SOA can be primarily

358 attributed to C₄₋₅ carbonyls and the “others” category (Fig. S14B and Fig. S15B).^{42,44} Nonaromatic
 359 nitro-substituted carbonyl chromophores, such as C₄H₃NO₇ in furan SOA,⁴⁴ may also contribute
 360 to BrC light absorption. Similarly, light absorption of furfural SOA can be mainly attributed to the
 361 carbonyl chromophores (Fig. S14C and Fig. S15C), which is likely related to the carbonyl
 362 functional group in furfural. Collectively, these findings demonstrate the significance of carbonyl
 363 chromophores in the light absorption of secondary BrC.



364
 365 **Figure 4.** Light absorption contribution of chromophores to MAC profiles: (A) C₄ carbonyls, C₄
 366 nitroaromatics and other chromophores in pyrrole SOA; (B) C₅ carbonyls, C₅ nitroaromatics and
 367 other chromophores in 2-MP SOA.
 368



369

370 **Figure 5.** Light absorption contributions of maleimide to (A) pyrrole SOA and (B) 1-MP SOA,
 371 and phthalic anhydride to (C) furan SOA and (D) furfural SOA under low and high NO_3 levels.
 372 The absorption contribution is estimated by the ratio of light absorption of molecular
 373 chromophores calculated by the Beer-Lambert law and the total light absorption of BrC samples.
 374 The shadow around the lines shows the standard deviation of absorption contribution at each
 375 wavelength.

376

377 Furthermore, depending on the SOA systems, the light absorption contribution of
 378 molecular carbonyl chromophores in secondary BrC may vary under different environmental
 379 conditions. The NO_3 radical level has been reported as a critical environmental factor that affects
 380 the secondary BrC formation of pyrroles and furans.⁴²⁻⁴⁴ As marker compounds of secondary BrC
 381 from the nighttime oxidation of several unsaturated heterocyclic VOC precursors, maleimide and
 382 phthalic anhydride were selected to investigate the influence of NO_3 radical levels on their light
 383 absorption contribution, and their molecular light absorptivity and mass ratio in various SOA

samples have been experimentally measured in prior studies.⁴³ Our results indicated that the light absorption contribution of maleimide in pyrrole SOA remained essentially constant as the NO₃ radical level increased (Fig. 5A), whereas it increased significantly in 1-MP SOA as the nitrate radical level increased (Fig. 5B). The light absorption contribution of phthalic anhydride exhibited a divergent trend in furan SOA and in furfural SOA as the NO₃ radical level increased; specifically, it reduced in furan SOA and enhanced in furfural SOA (Fig. 5C-D). The dependence of light absorption contribution on the level of NO₃ radicals may be attributed to the alteration of chemical kinetics and, consequently, the branching ratios of carbonyl chromophores production as the NO₃ concentrations change. The effects of VOC types on the contribution of molecular carbonyl chromophores to light absorption should also be noted. Maleimide, for instance, may account for ~7% of light absorption at 290 nm in pyrrole SOA (Fig. 5A), but a much lower value in 1-MP SOA (Fig. 5B). The observed discrepancy could be attributed to the methyl group on 1-MP, which could hinder the formation of maleimide and alternatively generate other chromophores (e.g., N-methylmaleimide in Fig. 3D). Thus, the role of carbonyl chromophores in secondary BrC is significantly influenced by complex atmospheric conditions and VOC emissions.

Overall, our results indicate the prevalence of carbonyl chromophores in SOA from the nighttime oxidation of heterocyclic VOCs. The UV-Vis spectra of the characterized carbonyl chromophores cover a wider range of wavelengths (i.e., ~290-500 nm) compared to the nitroaromatic chromophores (i.e., ~290-400 nm) characterized in our previous studies,^{42, 55} suggesting their distinct contributions to BrC light absorption at different wavelengths. Comparison between isomers also highlights that the spectral light absorptivity of carbonyl chromophores in secondary BrC can be governed by the structure of VOC precursors, which is consistent with our previous research on nitroaromatic chromophores.⁴² The structural dependence

407 of UV-Vis spectra indicates the importance of structure-related information in the process-level
408 prediction of secondary BrC formation. Moreover, the characterized carbonyl chromophores and
409 their structural analogues, including heterocyclic diones and triones, have been widely observed
410 in SOA systems from other VOCs, for example, those generated by photooxidation of a variety of
411 aromatic hydrocarbons.⁵⁹⁻⁶³ Heterocyclic diones have also been widely observed in field
412 measurements of ambient aerosols from biomass burning plumes.^{38, 64, 65} Although triones in
413 ambient aerosols were less reported,⁶⁶ they have been suggested as possible contributors to BrC
414 generated from aqueous-phase reactions.^{67, 68} The collective evidence demonstrates that carbonyl
415 chromophores are ubiquitous constituents in SOA and may play an active role in secondary BrC
416 formation.

417

418 **ATMOSPHERIC IMPLICATIONS**

419 Molecular chromophores are the key to BrC light absorption, connecting the microscopic
420 physicochemical processes in atmospheric aerosols with the macroscopic radiative budget in the
421 Earth system. The newly characterized chromophores enable a more detailed process-level
422 depiction of BrC formation, which is essential for improving the assessment of BrC's impact in
423 the context of climate change. Our study shows that carbonyl chromophores can be important
424 constituents of secondary BrC from nighttime oxidation of heterocyclic VOCs, with wavelengths
425 ranging from UV to visible. While research on ambient aerosols in wildfires has suggested that
426 nitroaromatic chromophores, such as nitrophenols, nitrocatechols, nitroguaiacols, and
427 nitrosyringols, may predominately contribute to BrC light absorption in the visible range,^{16, 17} field
428 studies have also provided increasing evidence indicating that carbonyl chromophores could be
429 distinct contributors to BrC light absorption in the UV range.⁶⁹ It is further noted that the carbonyl

430 chromophores characterized in our studies are not only found in other SOA systems but are also
431 commonly observed in field studies.^{38, 59-65} Indeed, carbonyl compounds are ubiquitous in
432 atmospheric aerosols and have long been recognized as the key species in tropospheric chemistry^{70,}
433 ⁷¹ and the critical precursors of secondary BrC formation in the aerosol phase via NH₃/amine-
434 driven reactions⁷²⁻⁷⁵ or forming charge transfer complexes with alcohols.^{76, 77} Our study can
435 complementarily provide a new perspective for evaluating the role of carbonyls in atmospheric
436 aerosols based on their intrinsic light absorption, for example, the initiation of photosensitization
437 which can facilitate aqueous SOA formation.⁷⁸⁻⁸²

438 Furthermore, carbonyl chromophores produced by nighttime oxidation of N-containing
439 VOCs may represent a potentially important component in secondary BrC that was previously
440 unrecognized. Our study reveals that light-absorbing imides and amides can be critical
441 chromophores in the SOA of pyrrole and its derivatives. Given that biomass burning releases a
442 variety of N-containing heterocyclic VOC precursors,³⁷⁻³⁹ the formation of N-containing carbonyl
443 chromophores could be a potentially significant contributor to the light absorption of secondary
444 BrC. Furthermore, as widely observed in field studies of wildfire emissions,^{33, 38, 83, 84} N-containing
445 carbonyl chromophores offer another pivot in addition to the nitroaromatic chromophores for a
446 more in-depth understanding of secondary BrC formation, particularly the wavelength-dependent
447 change of BrC light absorption as well as the diverse physicochemical processes. Although
448 nitroaromatic chromophores may likely possess stronger absorptivity compared to carbonyl
449 chromophores, the former are largely related to anthropogenic emissions of NO_x,^{85, 86} whereas the
450 latter may be generated by more divergent atmospheric oxidation pathways, such as OH-driven
451 oxidation of VOCs.⁶⁴ Broader sources of carbonyl chromophores may result in greater ubiquity in
452 the atmosphere under different environmental conditions, implying more extensive effects. Further

453 research is needed to reveal the role of carbonyl chromophores in other BrC systems and to
454 estimate the radiative forcing from carbonyl chromophores. Overall, this study expands the current
455 understanding of chromophore formation and provides a molecular-level foundation as the basis
456 for further investigations into the effects of secondary BrC formation on the Earth's energy budget
457 in the context of climate change.

458

459 ASSOCIATED CONTENT

460 Supporting Information

461 ACN extraction efficiency of surrogate standards of BrC chromophores (Table S1); Cartesian
462 coordinates for geometrical structures of carbonyl chromophores in the theoretical calculations
463 (Table S2); Wavelength-dependent EF_{absC} of C₄₋₅ carbonyls and C₄₋₅ nitroaromatics (Table S3);
464 First-order wall loss rate constants along with particulate diameter (Figure S1); LC mobile phase
465 composition along with retention time and response factors of selected N-containing carbonyls
466 (Figure S2); LC-DAD heatmap and compositional mass spectra of 2-MP SOA (Figure S3); LC-
467 DAD heatmaps and compositional mass spectra of 1-MP SOA (Figure S4); LC-DAD heatmaps
468 and compositional mass spectra of furfural SOA (Figure S5); Tentative fragmentation pathways
469 of C₄H₄NO₄⁻ and C₄HO₄⁻ (Figure S6); Heterocyclic carbonyl chromophores in pyrrole SOA
470 (Figure S7); Tentative fragmentation pathways of C₄H₂NO₃⁻ (Figure S8); Tentative fragmentation
471 pathways of C₄H₂NO₄⁻ (Figure S9); Tentative fragmentation pathways of C₄H₄NO₃⁻ (Figure S10);
472 Tentative fragmentation pathways of C₅H₅NO₂ (Figure S11); Oxidation products with higher
473 molecular weights and high double bond equivalence (Figure S12); Light absorption contributions
474 of chromophores in pyrrole SOA and 2-MP SOA in percentages (Figure S13); Light absorption
475 contributions of chromophores in 1-MP SOA, furan SOA and furfural SOA in percentages (Figure

476 S14); Light absorption contributions of chromophores to the MAC profiles in 1-MP SOA, furan
477 SOA and furfural SOA (Figure S15).

478

479 **AUTHOR INFORMATION**

480 **Corresponding Author**

481 * Phone: +1-951-827-3785. E-mail: ying-hsuan.lin@ucr.edu

482 **Notes**

483 The authors declare no competing financial interest.

484

485 **ACKNOWLEDGEMENTS**

486 This work was supported by NSF AGS-1953905 and the UCR Hellman Fellowship granted to
487 Ying-Hsuan Lin. We thank Dr. Jie Zhou at UCR Analytical Chemistry Instrumentation Facility
488 (ACIF) for their assistance with UPLC-DAD-ESI-Q-TOFMS (supported by NSF CHE-0541848).

489 **REFERENCE**

490 1. Lin, G.; Penner, J. E.; Flanner, M. G.; Sillman, S.; Xu, L.; Zhou, C., Radiative forcing of
491 organic aerosol in the atmosphere and on snow: Effects of SOA and brown carbon. *J. Geophys. Res. Atmos.* **2014**, *119*, (12), 7453-7476.

493 2. Feng, Y.; Ramanathan, V.; Kotamarthi, V. R., Brown carbon: a significant atmospheric
494 absorber of solar radiation? *Atmospheric chemistry and physics* **2013**, *13*, (17), 8607-8621.

495 3. Zhang, A.; Wang, Y.; Zhang, Y.; Weber, R. J.; Song, Y.; Ke, Z.; Zou, Y., Modeling the
496 global radiative effect of brown carbon: a potentially larger heating source in the tropical free
497 troposphere than black carbon. *Atmos. Chem. Phys.* **2020**, *20*, (4), 1901-1920.

498 4. Liu, J.; Scheuer, E.; Dibb, J.; Ziembka, L. D.; Thornhill, K. L.; Anderson, B. E.; Wisthaler,
499 A.; Mikoviny, T.; Devi, J. J.; Bergin, M.; Weber, R. J., Brown carbon in the continental
500 troposphere. *Geophys. Res. Lett.* **2014**, *41*, (6), 2191-2195.

501 5. Zhang, Y.; Forrister, H.; Liu, J.; Dibb, J.; Anderson, B.; Schwarz, J. P.; Perring, A. E.;
502 Jimenez, J. L.; Campuzano-Jost, P.; Wang, Y.; Nenes, A.; Weber, R. J., Top-of-atmosphere
503 radiative forcing affected by brown carbon in the upper troposphere. *Nature Geoscience* **2017**,
504 *10*, (7), 486-489.

505 6. Zhao, S.; Qi, S.; Yu, Y.; Kang, S.; Dong, L.; Chen, J.; Yin, D., Measurement report:
506 Contrasting elevation-dependent light absorption by black and brown carbon: lessons from in
507 situ measurements from the highly polluted Sichuan Basin to the pristine Tibetan Plateau. *Atmos.*
508 *Chem. Phys.* **2022**, *22*, (22), 14693-14708.

509 7. Ferrero, L.; Močnik, G.; Cogliati, S.; Gregorič, A.; Colombo, R.; Bolzacchini, E.,
510 Heating Rate of Light Absorbing Aerosols: Time-Resolved Measurements, the Role of Clouds,
511 and Source Identification. *Environ. Sci. Technol.* **2018**, *52*, (6), 3546-3555.

512 8. Tian, P.; Liu, D.; Zhao, D.; Yu, C.; Liu, Q.; Huang, M.; Deng, Z.; Ran, L.; Wu, Y.; Ding,
513 S.; Hu, K.; Zhao, G.; Zhao, C.; Ding, D., In situ vertical characteristics of optical properties and
514 heating rates of aerosol over Beijing. *Atmos. Chem. Phys.* **2020**, *20*, (4), 2603-2622.

515 9. Brown, H.; Liu, X.; Feng, Y.; Jiang, Y.; Wu, M.; Lu, Z.; Wu, C.; Murphy, S.; Pokhrel,
516 R., Radiative effect and climate impacts of brown carbon with the Community Atmosphere
517 Model (CAM5). *Atmospheric chemistry and physics* **2018**, *18*, (24), 17745-17768.

518 10. Xu, J.; Hettiyadura, A. P. S.; Liu, Y.; Zhang, X.; Kang, S.; Laskin, A., Atmospheric
519 Brown Carbon on the Tibetan Plateau: Regional Differences in Chemical Composition and Light
520 Absorption Properties. *Environmental Science & Technology Letters* **2022**, *9*, (3), 219-225.

521 11. Liu, D.; He, C.; Schwarz, J. P.; Wang, X., Lifecycle of light-absorbing carbonaceous
522 aerosols in the atmosphere. *npj Climate and Atmospheric Science* **2020**, *3*, (1), 40.

523 12. Laskin, A.; Laskin, J.; Nizkorodov, S. A., Chemistry of Atmospheric Brown Carbon.
524 *Chem. Rev.* **2015**, *115*, (10), 4335-4382.

525 13. Moise, T.; Flores, J. M.; Rudich, Y., Optical Properties of Secondary Organic Aerosols
526 and Their Changes by Chemical Processes. *Chem. Rev.* **2015**, *115*, (10), 4400-4439.

527 14. Li, X.; Wang, Y.; Hu, M.; Tan, T.; Li, M.; Wu, Z.; Chen, S.; Tang, X., Characterizing
528 chemical composition and light absorption of nitroaromatic compounds in the winter of Beijing.
529 *Atmos. Environ.* **2020**, *237*, 117712.

530 15. Frka, S.; Šala, M.; Brodnik, H.; Štefane, B.; Kroflič, A.; Grgić, I., Seasonal variability of
531 nitroaromatic compounds in ambient aerosols: Mass size distribution, possible sources and
532 contribution to water-soluble brown carbon light absorption. *Chemosphere* **2022**, *299*, 134381.

533 16. Bluvshstein, N.; Lin, P.; Flores, J. M.; Segev, L.; Mazar, Y.; Tas, E.; Snider, G.; Weagle, C.; Brown, S. S.; Laskin, A.; Rudich, Y., Broadband optical properties of biomass-burning aerosol and identification of brown carbon chromophores. *J. Geophys. Res. Atmos.* **2017**, *122*, (10), 5441-5456.

537 17. Lin, P.; Bluvshstein, N.; Rudich, Y.; Nizkorodov, S. A.; Laskin, J.; Laskin, A., Molecular 538 Chemistry of Atmospheric Brown Carbon Inferred from a Nationwide Biomass Burning Event. 539 *Environ. Sci. Technol.* **2017**, *51*, (20), 11561-11570.

540 18. Xie, M.; Hays, M. D.; Holder, A. L., Light-absorbing organic carbon from prescribed and 541 laboratory biomass burning and gasoline vehicle emissions. *Scientific Reports* **2017**, *7*, (1), 7318.

542 19. Li, X.; Hu, M.; Wang, Y.; Xu, N.; Fan, H.; Zong, T.; Wu, Z.; Guo, S.; Zhu, W.; Chen, S.; 543 Dong, H.; Zeng, L.; Yu, X.; Tang, X., Links between the optical properties and chemical 544 compositions of brown carbon chromophores in different environments: Contributions and 545 formation of functionalized aromatic compounds. *Sci. Total Environ.* **2021**, *786*, 147418.

546 20. Wang, Z.; Zhang, J.; Zhang, L.; Liang, Y.; Shi, Q., Characterization of nitroaromatic 547 compounds in atmospheric particulate matter from Beijing. *Atmos. Environ.* **2020**, 118046.

548 21. Zhao, R.; Lee, A. K. Y.; Huang, L.; Li, X.; Yang, F.; Abbatt, J. P. D., Photochemical 549 processing of aqueous atmospheric brown carbon. *Atmos. Chem. Phys.* **2015**, *15*, (11), 6087- 550 6100.

551 22. Hems, R. F.; Abbatt, J. P. D., Aqueous Phase Photo-oxidation of Brown Carbon 552 Nitrophenols: Reaction Kinetics, Mechanism, and Evolution of Light Absorption. *ACS Earth 553 Space Chem.* **2018**, *2*, (3), 225-234.

554 23. Braman, T.; Dolvin, L.; Thrasher, C.; Yu, H.; Walhout, E. Q.; O'Brien, R. E., Fresh 555 versus Photo-recalcitrant Secondary Organic Aerosol: Effects of Organic Mixtures on Aqueous 556 Photodegradation of 4-Nitrophenol. *Environmental Science & Technology Letters* **2020**, *7*, (4), 557 248-253.

558 24. Wang, Y.; Huang, W.; Tian, L.; Wang, Y.; Li, F.; Huang, D. D.; Zhang, R.; Go Mabato, B. R.; Huang, R.-J.; Chen, Q.; Ge, X.; Du, L.; Ma, Y. G.; Gen, M.; Hoi, K. I.; Mok, K. M.; Yu, J. Z.; Chan, C. K.; Li, X.; Li, Y. J., Decay Kinetics and Absorption Changes of Methoxyphenols 559 and Nitrophenols during Nitrate-Mediated Aqueous Photochemical Oxidation at 254 and 313 560 nm. *ACS Earth Space Chem.* **2022**, *6*, (4), 1115-1125.

561 25. Yang, J.; Au, W. C.; Law, H.; Leung, C. H.; Lam, C. H.; Nah, T., pH affects the aqueous- 562 phase nitrate-mediated photooxidation of phenolic compounds: implications for brown carbon 563 formation and evolution. *Environ. Sci. Process Impacts* **2022**.

564 26. Witkowski, B.; Jain, P.; Gierczak, T., Aqueous chemical bleaching of 4-nitrophenol 565 brown carbon by hydroxyl radicals; products, mechanism, and light absorption. *Atmos. Chem. 566 Phys.* **2022**, *22*, (8), 5651-5663.

567 27. Xie, M.; Chen, X.; Hays, M. D.; Lewandowski, M.; Offenberg, J.; Kleindienst, T. E.; 568 Holder, A. L., Light Absorption of Secondary Organic Aerosol: Composition and Contribution 569 of Nitroaromatic Compounds. *Environ. Sci. Technol.* **2017**, *51*, (20), 11607-11616.

570 28. McNeill, V. F., Atmospheric Aerosols: Clouds, Chemistry, and Climate. *Annual Review 571 of Chemical and Biomolecular Engineering* **2017**, *8*, (1), 427-444.

572 29. Gardner, E. P.; Sperry, P. D.; Calvert, J. G., Photodecomposition of acrolein in oxygen- 573 nitrogen mixtures. *J. Phys. Chem.* **1987**, *91*, (7), 1922-1930.

574 30. Magneron, I.; Thévenet, R.; Mellouki, A.; Le Bras, G.; Moortgat, G. K.; Wirtz, K., A 575 Study of the Photolysis and OH-initiated Oxidation of Acrolein and trans-Crotonaldehyde. *J. 576 Phys. Chem. A* **2002**, *106*, (11), 2526-2537.

577

578

579 31. Mayol-Bracero, O. L.; Guyon, P.; Graham, B.; Roberts, G.; Andreae, M. O.; Decesari, S.;
580 Facchini, M. C.; Fuzzi, S.; Artaxo, P., Water-soluble organic compounds in biomass burning
581 aerosols over Amazonia 2. Apportionment of the chemical composition and importance of the
582 polyacidic fraction. *Journal of Geophysical Research: Atmospheres* **2002**, *107*, (D20), LBA 59-
583 1-LBA 59-15.

584 32. Garcia-Hurtado, E.; Pey, J.; Borrás, E.; Sánchez, P.; Vera, T.; Carratalá, A.; Alastuey, A.;
585 Querol, X.; Vallejo, V. R., Atmospheric PM and volatile organic compounds released from
586 Mediterranean shrubland wildfires. *Atmos. Environ.* **2014**, *89*, 85-92.

587 33. Zhou, Y.; West, C. P.; Hettiyadura, A. P. S.; Pu, W.; Shi, T.; Niu, X.; Wen, H.; Cui, J.;
588 Wang, X.; Laskin, A., Molecular Characterization of Water-Soluble Brown Carbon
589 Chromophores in Snowpack from Northern Xinjiang, China. *Environ. Sci. Technol.* **2022**, *56*,
590 (7), 4173-4186.

591 34. Desyaterik, Y.; Sun, Y.; Shen, X.; Lee, T.; Wang, X.; Wang, T.; Collett Jr, J. L.,
592 Speciation of “brown” carbon in cloud water impacted by agricultural biomass burning in eastern
593 China. *J. Geophys. Res. Atmos.* **2013**, *118*, (13), 7389-7399.

594 35. Jacobson, M. Z., Isolating nitrated and aromatic aerosols and nitrated aromatic gases as
595 sources of ultraviolet light absorption. *J. Geophys. Res. Atmos.* **1999**, *104*, (D3), 3527-3542.

596 36. Karl, T. G.; Christian, T. J.; Yokelson, R. J.; Artaxo, P.; Hao, W. M.; Guenther, A., The
597 Tropical Forest and Fire Emissions Experiment: method evaluation of volatile organic compound
598 emissions measured by PTR-MS, FTIR, and GC from tropical biomass burning. *Atmos. Chem. Chem.*
599 *Phys.* **2007**, *7*, (22), 5883-5897.

600 37. Hatch, L. E.; Luo, W.; Pankow, J. F.; Yokelson, R. J.; Stockwell, C. E.; Barsanti, K. C.,
601 Identification and quantification of gaseous organic compounds emitted from biomass burning
602 using two-dimensional gas chromatography-time-of-flight mass spectrometry. *Atmos. Chem. Chem.*
603 *Phys.* **2015**, *15*, (4), 1865-1899.

604 38. Koss, A. R.; Sekimoto, K.; Gilman, J. B.; Selimovic, V.; Coggon, M. M.; Zarzana, K. J.;
605 Yuan, B.; Lerner, B. M.; Brown, S. S.; Jimenez, J. L.; Krechmer, J.; Roberts, J. M.; Warneke, C.;
606 Yokelson, R. J.; de Gouw, J., Non-methane organic gas emissions from biomass burning:
607 identification, quantification, and emission factors from PTR-ToF during the FIREX 2016
608 laboratory experiment. *Atmos. Chem. Phys.* **2018**, *18*, (5), 3299-3319.

609 39. Andreae, M. O., Emission of trace gases and aerosols from biomass burning – an updated
610 assessment. *Atmos. Chem. Phys.* **2019**, *19*, (13), 8523-8546.

611 40. Decker, Z. C. J.; Zarzana, K. J.; Coggon, M.; Min, K.-E.; Pollack, I.; Ryerson, T. B.;
612 Peischl, J.; Edwards, P.; Dubé, W. P.; Markovic, M. Z.; Roberts, J. M.; Veres, P. R.; Graus, M.;
613 Warneke, C.; de Gouw, J.; Hatch, L. E.; Barsanti, K. C.; Brown, S. S., Nighttime Chemical
614 Transformation in Biomass Burning Plumes: A Box Model Analysis Initialized with Aircraft
615 Observations. *Environ. Sci. Technol.* **2019**, *53*, (5), 2529-2538.

616 41. Jiang, H.; Frie, A. L.; Lavi, A.; Chen, J. Y.; Zhang, H.; Bahreini, R.; Lin, Y.-H., Brown
617 Carbon Formation from Nighttime Chemistry of Unsaturated Heterocyclic Volatile Organic
618 Compounds. *Environ. Sci. Technol. Lett.* **2019**, *6*, (3), 184-190.

619 42. Mayorga, R.; Chen, K.; Raeofy, N.; Woods, M.; Lum, M.; Zhao, Z.; Zhang, W.;
620 Bahreini, R.; Lin, Y.-H.; Zhang, H., Chemical Structure Regulates the Formation of Secondary
621 Organic Aerosol and Brown Carbon in Nitrate Radical Oxidation of Pyrroles and
622 Methylpyrroles. *Environ. Sci. Technol.* **2022**, *56*, (12), 7761-7770.

623 43. Chen, K.; Raeofy, N.; Lum, M.; Mayorga, R.; Woods, M.; Bahreini, R.; Zhang, H.; Lin, Y.-H., Solvent effects on chemical composition and optical properties of extracted secondary brown carbon constituents. *Aerosol Sci. Tech.* **2022**, *56*, (10), 917-930.

624 44. Chen, K.; Mayorga, R.; Raeofy, N.; Lum, M.; Woods, M.; Bahreini, R.; Zhang, H.; Lin, Y.-H., Effects of Nitrate Radical Levels and Pre-Existing Particles on Secondary Brown Carbon

625 Formation from Nighttime Oxidation of Furan. *ACS Earth Space Chem.* **2022**, *6*, (11), 2709-2721.

626 45. Ziemann, P. J.; Atkinson, R., Kinetics, products, and mechanisms of secondary organic

627 aerosol formation. *Chem. Soc. Rev.* **2012**, *41*, (19), 6582-6605.

628 46. Lopez-Hilfiker, F. D.; Mohr, C.; Ehn, M.; Rubach, F.; Kleist, E.; Wildt, J.; Mentel, T. F.; Lutz, A.; Hallquist, M.; Worsnop, D.; Thornton, J. A., A novel method for online analysis of gas

629 and particle composition: description and evaluation of a Filter Inlet for Gases and AEROsols (FIGAERO). *Atmos. Meas. Tech.* **2014**, *7*, (4), 983-1001.

630 47. Zhang, X.; Zhang, H.; Xu, W.; Wu, X.; Tyndall, G. S.; Orlando, J. J.; Jayne, J. T.; Worsnop, D. R.; Canagaratna, M. R., Molecular characterization of alkyl nitrates in atmospheric

631 aerosols by ion mobility mass spectrometry. *Atmos. Meas. Tech.* **2019**, *12*, (10), 5535-5545.

632 48. Zhao, Z.; Yang, X.; Lee, J.; Tolentino, R.; Mayorga, R.; Zhang, W.; Zhang, H., Diverse

633 Reactions in Highly Functionalized Organic Aerosols during Thermal Desorption. *ACS Earth*

634 *Space Chem.* **2020**, *4*, (2), 283-296.

635 49. Mayorga, R. J.; Zhao, Z.; Zhang, H., Formation of secondary organic aerosol from nitrate

636 radical oxidation of phenolic VOCs: Implications for nitration mechanisms and brown carbon

637 formation. *Atmos. Environ.* **2021**, *244*, 117910.

638 50. Frisch, M. J.; Trucks, G. W.; Schlegel, H. B.; Scuseria, G. E.; Robb, M. A.; Cheeseman,

639 J. R.; Scalmani, G.; Barone, V.; Petersson, G. A.; Nakatsuji, H.; Li, X.; Caricato, M.; Marenich,

640 A. V.; Bloino, J.; Janesko, B. G.; Gomperts, R.; Mennucci, B.; Hratchian, H. P.; Ortiz, J. V.; Izmaylov, A. F.; Sonnenberg, J. L.; Williams; Ding, F.; Lippalini, F.; Egidi, F.; Goings, J.; Peng,

641 B.; Petrone, A.; Henderson, T.; Ranasinghe, D.; Zakrzewski, V. G.; Gao, J.; Rega, N.; Zheng, G.; Liang, W.; Hada, M.; Ehara, M.; Toyota, K.; Fukuda, R.; Hasegawa, J.; Ishida, M.; Nakajima, T.; Honda, Y.; Kitao, O.; Nakai, H.; Vreven, T.; Throssell, K.; Montgomery Jr., J. A.; Peralta, J. E.; Ogliaro, F.; Bearpark, M. J.; Heyd, J. J.; Brothers, E. N.; Kudin, K. N.; Staroverov, V. N.; Keith, T. A.; Kobayashi, R.; Normand, J.; Raghavachari, K.; Rendell, A. P.; Burant, J. C.; Iyengar, S. S.; Tomasi, J.; Cossi, M.; Millam, J. M.; Klene, M.; Adamo, C.; Cammi, R.; Ochterski, J. W.; Martin, R. L.; Morokuma, K.; Farkas, O.; Foresman, J. B.; Fox, D. J. *Gaussian 16 Rev. C.01*, Wallingford, CT, 2016.

642 51. Becke, A. D., Density-functional exchange-energy approximation with correct

643 asymptotic behavior. *Physical Review A* **1988**, *38*, (6), 3098-3100.

644 52. Stephens, P. J.; Devlin, F. J.; Chabalowski, C. F.; Frisch, M. J., Ab Initio Calculation of

645 Vibrational Absorption and Circular Dichroism Spectra Using Density Functional Force Fields.

646 *The Journal of Physical Chemistry* **1994**, *98*, (45), 11623-11627.

647 53. Ditchfield, R.; Hehre, W. J.; Pople, J. A., Self-Consistent Molecular-Orbital Methods.

648 IX. An Extended Gaussian-Type Basis for Molecular-Orbital Studies of Organic Molecules. *J. Chem. Phys.* **1971**, *54*, (2), 724-728.

649 54. Jacquemin, D.; Perpète, E. A.; Scuseria, G. E.; Ciofini, I.; Adamo, C., TD-DFT

650 Performance for the Visible Absorption Spectra of Organic Dyes: Conventional versus Long-

651 Range Hybrids. *J. Chem. Theory Comput.* **2008**, *4*, (1), 123-135.

668 55. Chen, J. Y.; Rodriguez, E.; Jiang, H.; Chen, K.; Frie, A.; Zhang, H.; Bahreini, R.; Lin,
669 Y.-H., Time-Dependent Density Functional Theory Investigation of the UV–Vis Spectra of
670 Organonitrogen Chromophores in Brown Carbon. *ACS Earth Space Chem.* **2020**, *4*, (2), 311-320.

671 56. Mennucci, B.; Cammi, R.; Tomasi, J., Excited states and solvatochromic shifts within a
672 nonequilibrium solvation approach: A new formulation of the integral equation formalism
673 method at the self-consistent field, configuration interaction, and multiconfiguration self-
674 consistent field level. *J. Chem. Phys.* **1998**, *109*, (7), 2798-2807.

675 57. Veblen, T. T.; Kitzberger, T.; Donnegan, J., Climatic and Human Influences on Fire
676 Regimes in Ponderosa Pine Forests in the Colorado Front Range. *Ecological Applications* **2000**,
677 *10*, (4), 1178-1195.

678 58. Zhang, W.; Wang, T.; Du, B.; Mu, L.; Feng, C., Mechanism for the gas-phase reaction
679 between NO₃ and furan: A theoretical study. *Chemical Physics Letters* **2008**, *455*, (4), 164-168.

680 59. Forstner, H. J. L.; Flagan, R. C.; Seinfeld, J. H., Secondary Organic Aerosol from the
681 Photooxidation of Aromatic Hydrocarbons: Molecular Composition. *Environ. Sci. Technol.*
682 **1997**, *31*, (5), 1345-1358.

683 60. Yu, J.; Jeffries, H. E.; Sexton, K. G., Atmospheric photooxidation of alkylbenzenes—I.
684 Carbonyl product analyses. *Atmos. Environ.* **1997**, *31*, (15), 2261-2280.

685 61. Edney, E. O.; Driscoll, D. J.; Weathers, W. S.; Kleindienst, T. E.; Conver, T. S.; McIver,
686 C. D.; Li, W., Formation of Polyketones in Irradiated Toluene/Propylene/NO x /Air Mixtures.
687 *Aerosol Sci. Tech.* **2001**, *35*, (6), 998-1008.

688 62. Hamilton, J. F.; Lewis, A. C.; Bloss, C.; Wagner, V.; Henderson, A. P.; Golding, B. T.;
689 Wirtz, K.; Martin-Reviejo, M.; Pilling, M. J., Measurements of photo-oxidation products from
690 the reaction of a series of alkyl-benzenes with hydroxyl radicals during EXACT using
691 comprehensive gas chromatography. *Atmos. Chem. Phys.* **2003**, *3*, (6), 1999-2014.

692 63. Lee, J. Y.; Lane, D. A., Unique products from the reaction of naphthalene with the
693 hydroxyl radical. *Atmos. Environ.* **2009**, *43*, (32), 4886-4893.

694 64. Coggon, M. M.; Lim, C. Y.; Koss, A. R.; Sekimoto, K.; Yuan, B.; Gilman, J. B.; Hagan,
695 D. H.; Selimovic, V.; Zarzana, K. J.; Brown, S. S.; Roberts, J. M.; Müller, M.; Yokelson, R.;
696 Wisthaler, A.; Krechmer, J. E.; Jimenez, J. L.; Cappa, C.; Kroll, J. H.; de Gouw, J.; Warneke, C.,
697 OH chemistry of non-methane organic gases (NMOGs) emitted from laboratory and ambient
698 biomass burning smoke: evaluating the influence of furans and oxygenated aromatics on ozone
699 and secondary NMOG formation. *Atmos. Chem. Phys.* **2019**, *19*, (23), 14875-14899.

700 65. Liang, Y.; Weber, R. J.; Misztal, P. K.; Jen, C. N.; Goldstein, A. H., Aging of Volatile
701 Organic Compounds in October 2017 Northern California Wildfire Plumes. *Environ. Sci.*
702 *Technol.* **2022**, *56*, (3), 1557-1567.

703 66. Edney, E. O.; Kleindienst, T. E.; Conver, T. S.; McIver, C. D.; Corse, E. W.; Weathers,
704 W. S., Polar organic oxygenates in PM2.5 at a southeastern site in the United States. *Atmos.*
705 *Environ.* **2003**, *37*, (28), 3947-3965.

706 67. De Haan, D. O.; Jansen, K.; Rynaski, A. D.; Sueme, W. R. P.; Torkelson, A. K.; Czer, E.
707 T.; Kim, A. K.; Rafla, M. A.; De Haan, A. C.; Tolbert, M. A., Brown Carbon Production by
708 Aqueous-Phase Interactions of Glyoxal and SO₂. *Environ. Sci. Technol.* **2020**, *54*, (8), 4781-
709 4789.

710 68. Al-Abadleh, H. A.; Rana, M. S.; Mohammed, W.; Guzman, M. I., Dark Iron-Catalyzed
711 Reactions in Acidic and Viscous Aerosol Systems Efficiently Form Secondary Brown Carbon.
712 *Environ. Sci. Technol.* **2021**, *55*, (1), 209-219.

713 69. Lin, P.; Aiona, P. K.; Li, Y.; Shiraiwa, M.; Laskin, J.; Nizkorodov, S. A.; Laskin, A.,
714 Molecular Characterization of Brown Carbon in Biomass Burning Aerosol Particles. *Environ.*
715 *Sci. Technol.* **2016**, *50*, (21), 11815-11824.

716 70. Carlier, P.; Hannachi, H.; Mouvier, G., The chemistry of carbonyl compounds in the
717 atmosphere—A review. *Atmos. Environ.* **1986**, *20*, (11), 2079-2099.

718 71. Lary, D. J.; Shallcross, D. E., Central role of carbonyl compounds in atmospheric
719 chemistry. *J. Geophys. Res. Atmos.* **2000**, *105*, (D15), 19771-19778.

720 72. Updyke, K. M.; Nguyen, T. B.; Nizkorodov, S. A., Formation of brown carbon via
721 reactions of ammonia with secondary organic aerosols from biogenic and anthropogenic
722 precursors. *Atmos. Environ.* **2012**, *63*, 22-31.

723 73. Kampf, C. J.; Jakob, R.; Hoffmann, T., Identification and characterization of aging
724 products in the glyoxal/ammonium sulfate system – implications for light-absorbing
725 material in atmospheric aerosols. *Atmos. Chem. Phys.* **2012**, *12*, (14), 6323-6333.

726 74. Kampf, C. J.; Filippi, A.; Zuth, C.; Hoffmann, T.; Opatz, T., Secondary brown carbon
727 formation via the dicarbonyl imine pathway: nitrogen heterocycle formation and synergistic
728 effects. *Phys. Chem. Chem. Phys.* **2016**, *18*, (27), 18353-18364.

729 75. Marrero-Ortiz, W.; Hu, M.; Du, Z.; Ji, Y.; Wang, Y.; Guo, S.; Lin, Y.; Gomez-
730 Hernandez, M.; Peng, J.; Li, Y.; Secrest, J.; Zamora, M. L.; Wang, Y.; An, T.; Zhang, R.,
731 Formation and Optical Properties of Brown Carbon from Small α -Dicarbonyls and Amines.
732 *Environ. Sci. Technol.* **2019**, *53*, (1), 117-126.

733 76. Phillips, S. M.; Smith, G. D., Light Absorption by Charge Transfer Complexes in Brown
734 Carbon Aerosols. *Environ. Sci. Technol. Lett.* **2014**, *1*, (10), 382-386.

735 77. Phillips, S. M.; Smith, G. D., Further Evidence for Charge Transfer Complexes in Brown
736 Carbon Aerosols from Excitation–Emission Matrix Fluorescence Spectroscopy. *J. Phys. Chem. A*
737 **2015**, *119*, (19), 4545-4551.

738 78. Smith, J. D.; Sio, V.; Yu, L.; Zhang, Q.; Anastasio, C., Secondary Organic Aerosol
739 Production from Aqueous Reactions of Atmospheric Phenols with an Organic Triplet Excited
740 State. *Environ. Sci. Technol.* **2014**, *48*, (2), 1049-1057.

741 79. Yu, L.; Smith, J.; Laskin, A.; Anastasio, C.; Laskin, J.; Zhang, Q., Chemical
742 characterization of SOA formed from aqueous-phase reactions of phenols with the triplet excited
743 state of carbonyl and hydroxyl radical. *Atmos. Chem. Phys.* **2014**, *14*, (24), 13801-13816.

744 80. George, C.; Brüggemann, M.; Hayeck, N.; Tiné, L.; Donaldson, J., Chapter 14 -
745 Interfacial Photochemistry. In *Physical Chemistry of Gas-Liquid Interfaces*, Faust, J. A.; House,
746 J. E., Eds. Elsevier: 2018; pp 435-457.

747 81. Mabato, B. R. G.; Lyu, Y.; Ji, Y.; Li, Y. J.; Huang, D. D.; Li, X.; Nah, T.; Lam, C. H.;
748 Chan, C. K., Aqueous secondary organic aerosol formation from the direct photosensitized
749 oxidation of vanillin in the absence and presence of ammonium nitrate. *Atmos. Chem. Phys.*
750 **2022**, *22*, (1), 273-293.

751 82. Mabato, B. R. G.; Li, Y. J.; Huang, D. D.; Wang, Y.; Chan, C. K., Comparison of
752 aqueous secondary organic aerosol (aqSOA) product distributions from guaiacol oxidation by
753 non-phenolic and phenolic methoxybenzaldehydes as photosensitizers in the absence and
754 presence of ammonium nitrate. *Atmos. Chem. Phys.* **2023**, *23*, (4), 2859-2875.

755 83. Permar, W.; Wang, Q.; Selimovic, V.; Wielgasz, C.; Yokelson, R. J.; Hornbrook, R. S.;
756 Hills, A. J.; Apel, E. C.; Ku, I. T.; Zhou, Y.; Sive, B. C.; Sullivan, A. P.; Collett Jr, J. L.;
757 Campos, T. L.; Palm, B. B.; Peng, Q.; Thornton, J. A.; Garofalo, L. A.; Farmer, D. K.;
758 Kreidenweis, S. M.; Levin, E. J. T.; DeMott, P. J.; Flocke, F.; Fischer, E. V.; Hu, L., Emissions

759 of Trace Organic Gases From Western U.S. Wildfires Based on WE-CAN Aircraft
760 Measurements. *J. Geophys. Res. Atmos.* **2021**, *126*, (11), e2020JD033838.

761 84. Hayden, K. L.; Li, S. M.; Liggio, J.; Wheeler, M. J.; Wentzell, J. J. B.; Leithead, A.;
762 Brickell, P.; Mittermeier, R. L.; Oldham, Z.; Mihele, C. M.; Staebler, R. M.; Moussa, S. G.;
763 Darlington, A.; Wolde, M.; Thompson, D.; Chen, J.; Griffin, D.; Eckert, E.; Ditto, J. C.; He, M.;
764 Gentner, D. R., Reconciling the total carbon budget for boreal forest wildfire emissions using
765 airborne observations. *Atmos. Chem. Phys.* **2022**, *22*, (18), 12493-12523.

766 85. Wang, Y.; Hu, M.; Wang, Y.; Zheng, J.; Shang, D.; Yang, Y.; Liu, Y.; Li, X.; Tang, R.;
767 Zhu, W.; Du, Z.; Wu, Y.; Guo, S.; Wu, Z.; Lou, S.; Hallquist, M.; Yu, J. Z., The formation of
768 nitro-aromatic compounds under high NO_x and anthropogenic VOC conditions in urban Beijing,
769 China. *Atmos. Chem. Phys.* **2019**, *19*, (11), 7649-7665.

770 86. Siemens, K.; Morales, A.; He, Q.; Li, C.; Hettiyadura, A. P. S.; Rudich, Y.; Laskin, A.,
771 Molecular Analysis of Secondary Brown Carbon Produced from the Photooxidation of
772 Naphthalene. *Environ. Sci. Technol.* **2022**, *56*, (6), 3340-3353.

773